Contribution from the Department of Chemistry,
The University of Chicago, Chicago, Illinois 60637

Structures of Chevrel Phases

JEREMY K. BURDETT*[1] and JUNG-HUI LIN

Received March 16, 1981

The results of both molecular orbital and band structure calculations are used to understand the geometry of the Chevrel phases MM'_6X_{8-y} (M = Pb, Sn, Ba, Ag, Ln; M' = Ru, Mo, Rh; X = S, Se, Te; y = 0–2). The observed structures, an M'_6 octahedron within an X_8 cube (for y = 0) within a cube of M atoms, are somewhat distorted so as to relieve nonbonded repulsions between the closed shell X_8 units in adjacent unit cells. When $y \neq 0$, it is shown how it is the atoms in the special positions which are predicted to be missing in agreement with experiment. A larger turn angle in Chevrel phases where M is an electropositive atom is calculated, and it is suggested that this may have important bearing on high-temperature superconductivity.

Introduction

The ternary molybdenum chalconides, MMo_6X_y (Chevrel phases[2]), are known where M may be one of a variety of metals (Sn, Pb, Ba, Ag, Cu, Ln, etc.) and X is one of the chalcogens S, Se, or Te. Some examples of substitution of Mo by Rh or Ru are also known. These compounds have attracted interest because they havve curious structures and extraordinary[3,4] electrical and magnetic properties being high-temperature superconductors (~13 K for $Pb_{0.92}$, $Mo_6S_{7.5}$). The crystal structure of one of these compounds[5] (with y = 8) is shown in Figure 1 although it has proven difficult to grow single crystals of many of these materials. Eight X atoms form a nearly perfect cube and six Mo atoms nearly occupy the centers of the six square faces. Together these metal atoms form a slightly distorted octahedron. This Mo_6X_8 unit is contained within a larger cube of M atoms such that the three polyhedra we have mentioned share a common threefold rotation axis. The two X atoms which lie on this axis (special positions) are thus chemically distinguishable from the other six which lie in general positions. When y = 6, 7, either one or both of the atoms in the special positions are left out.

Thus the ideal structure is a high-symmetry one and may be described as an octahedron, within a cube, within a cube, all three polyhedra sharing a common centroid (**1**). In the

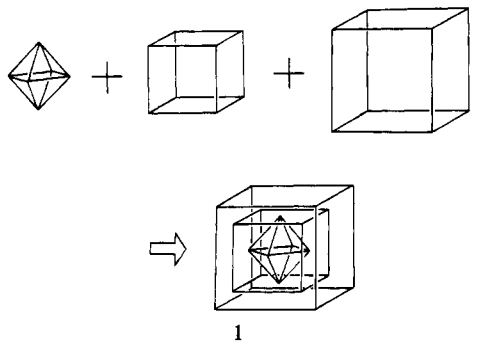

1

real structure the inner pair of polyhedra are rotated about a common threefold axis. The turn angle (ϕ) in the lead-containing examples is around 25°. The Mo_6X_8 arrangement itself is one which is well-known[6] in molecular chemistry as the $Mo_6Cl_8^{4+}$ ion (**2**) in "$MoCl_2$". In the Chevrel phases each

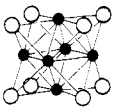

2

M atom is approximately cubally coordinated by X with two short and six longer M–X distances. Each X atom is tetrahedrally coordinated by three Mo atoms and one M atom. These X atoms in the special positions have shorter M–X distances and a more regular coordination than those in the general positions.

Theoretical studies exist[3,7] concerning the electrical and magnetic properties of these systems. In this paper we present a theoretical analysis of some geometrical aspects. We use results from molecular orbital calculations both on simple molecular fragments torn from the crystal lattice and from solid-state repeat units with cyclic boundary conditions imposed to mimic the solid-state environment.[8,9] We also use the results of band structure calculations for this solid-state problem. All the calculations employ the extended Hückel method.[10] The same atomic parameters are used throughout; their values are given in the Appendix. We will use both idealized and real geometries of $PbMo_6S_8$ for our model system. (See Appendix.)

Results of Molecular Calculations

We shall build up this structure in the following way (**1**) in order to understand in as transparent way as possible the electronic features of the species: (a) assemble an Mo_6 octahedron from six Mo atoms; (b) add the cube of eight X atoms to cover each octahedral face; (c) place this unit within a cube of M atoms such that the six pairs of faces of the two cubes are parallel; (d) allow rotation around one threefold cubal axis. For the Mo_6 and Mo_6X_8 units, we can perform molecular orbital calculations on these molecular units and also band structure calculations on a hypothetical infinite solid made up of such building blocks. For the final structure containing the cube of M atoms, "molecular" calculations on a $M_8Mo_6X_8$ unit are, of course, inappropriate (among other things, the stoichiometry is incorrect), and so in addition to band structure computations we have imposed cyclic boundary conditions on a molecular calculation for MMo_6X_8. (This is

(1) Fellow of the Alfred P. Sloan Foundation and Camille and Henry Dreyfus Teacher-Scholar.
(2) (a) Chevrel, R.; Sergent, M.; Prigent, J. *J. Solid State Chem.* **1971**, *3*, 315. (b) For an excellent review see: Fischer, Ø. *Appl. Phys.* **1978**, *16*, 1.
(3) (a) Andersen, O. K.; Klose, W.; Nohl, H. *Phys. Rev. B* **1978**, *17*, 1209. (b) Bullett, D. W. *Phys. Rev. Lett.* **1977**, *39*, 664.
(4) (a) Fischer, O; Jones, N.; Bongi, G.; Sergent, M.; Chevrel, R. *J. Phys. C* **1974**, *7*, L450. (b) Delk, F. S.; Sienko, M. J. *Inorg. Chem.* **1980**, *19*, 1352.
(5) (a) Marezio, M.; Dernier, P. D.; Remeika, J. P.; Corenzwit, E.; Matthias, B. T. *Mater. Res. Bull.* **1973**, *8*, 657. (b) Chevrel, R.; Sergent, M.; Prigent, J. *Ibid.* **1974**, *9*, 1487. (c) Bars, O.; Guillevic, J.; Grandjean, D. *J. Solid State Chem.* **1973**, *6*, 48. (d) Delk, F. S.; Sienko, M. J. *Inorg. Chem.* **1980**, *18*, 788. (e) Perrin, A.; Chevrel, R.; Sergent, M.; Fischer, Ø. *J. Solid State Chem.* **1980**, *33*, 43.
(6) (a) Cotton, F. A.; Haas, T. E. *Inorg. Chem.* **1964**, *3* 10. (b) Guggenberger, L. J.; Sleight, A. W. *Inorg. Chem.* **1969**, *8*, 2041.
(7) Mattheis, L. F.; Fong, C. Y. *Phys. Rev. B* **1977**, *15*, 1760.
(8) Burdett, J. K. *J. Am. Chem. Soc.* **1980**, *102*, 5458.
(9) Zunger, A. *J. Phys. C* **1974**, *7*, 96.
(10) (a) Hoffmann, R. *J. Chem. Phys.* **1963**, *39* 1397. (b) Hoffmann, R.; Lipscomb, W. N. *J. Chem. Phys.* **1962**, *36*, 3489.

0020-1669/82/1321-0005$01.25/0

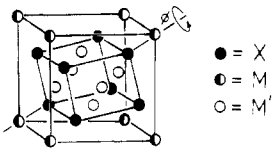

Figure 1. Crystal structure of a Chevrel phase. (Sometimes some of the atoms of the chalcogen cube are absent.)

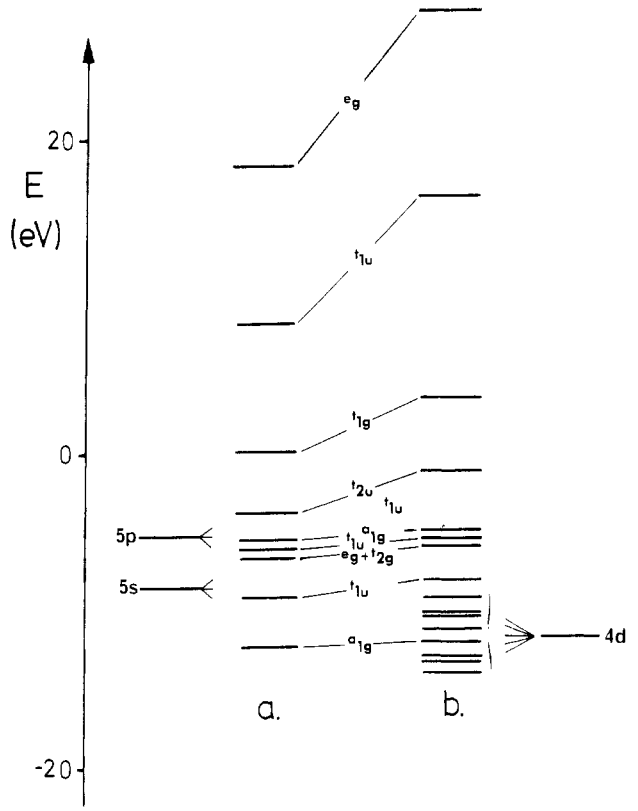

Figure 2. Orbital diagram for the Mo_6 cluster (a) without and (b) with d orbitals. The orbitals contained by the brace are (with the exception of the labeled a_{1g} orbital) largely d in character.

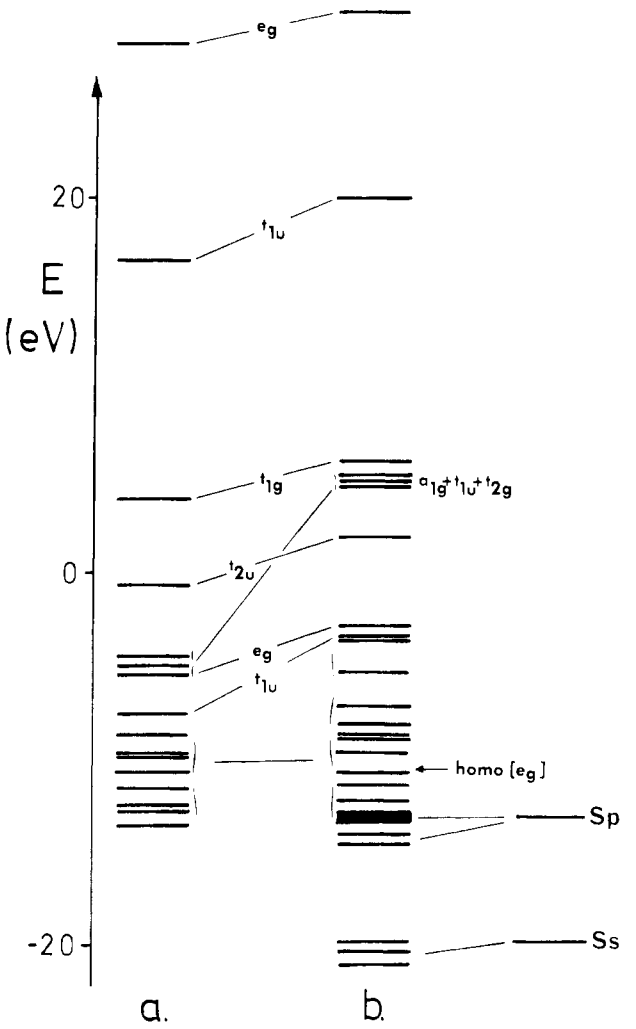

Figure 3. Generation of an orbtial diagram for Mo_6S_8 (b) from Mo_6 (a). The orbitals contained by the brace are largely d in character. The solid block of orbitals are largely sulfur 3p. The HOMO is indicated for $Mo_6S_8^{4-}$.

the fragment-within-the-solid[8] or small periodic cluster[9] approach.) Although there are 15 atoms and 90 valence atomic orbitals in the unit cell (ignoring d functions on the chalcogens), because of the high symmetry of the problem, a particularly simple orbital picture emerges. even so, for reasons of computational economy, the band structure calculations on MMo_6X_8 itself ignore the Mo d orbitals, although they are included in the pseudomolecular calculations.

Mo_6 Cluster. Figure 2a shows the derivation of the energy diagram for an isolated Mo_6 octahedral cluster where d orbitals have been excluded. The orbital pattern is just what is expected from use of the results[11] of the "$(n + 1)$ rule". There are a total of seven skeletal bonding orbitals ($a_{1g} + t_{1u} + t_{2g}$) although the t_{2g} orbital is not strongly bonding. The next highest set of orbitals are outward pointing ($a_{1g} + e_g + t_{1u}$) and approximately nonbonding. These are the orbitals which we expect to be prominent in interaction with those of the X_8 cube. The remaining 11 orbitals are antibonding. The molybdenum 4d orbitals are almost certainly important in influencing the electric and magnetic properties of these materials. The effect of their inclusion is shown in Figure 2b. The d-orbital manifold spans a region from −14.0 to −9.0 eV. The s,p manifold lies higher with the exception that the bonding a_{1g} orbital lies within the d orbital region. For an Mo_6^{12+} cluster all the valence electrons are associated with orbitals which are predominantly d in character, and the HOMO appears to be approximately nonbonding in character.

Mo_6X_8 Cluster. Figure 3 shows the energy levels of the Mo_6X_8 cluster. The molecular orbitals arising from the sulfur 3s and 3p orbitals are well separated in energy from the metal-located orbitals. The diagram is similar to those derived in previous studies[6] on the $Mo_6Cl_6^{4+}$ species, isoelectronic with an $Mo_6S_8^{4-}$ cluster. (For this reason our discussion is rather cursory.) Indeed with this electronic configuration a HOMO–LUMO gap of about 1 eV develops in our Mo_6X_8 calculation. The largest energetic changes ($Mo_6 \rightarrow Mo_6X_8$) are naturally associated with the outward-pointing orbitals of the clusters. The d group of orbitals in Mo_6 is broadened considerably when the faces are capped. The HOMO of e_g symmetry is located within this manifold or predominantly d orbitals.

MMo_6X_8. The derivation of the fragment-within-the-solid orbitals[8] for the $\phi = 0°$ MMo_6X_8 unit is very simple indeed. The metal atoms, M, lie at sites of cubal symmetry and so ns and np orbitals transform as $a_{1g} + t_{1u}$. Thus it is only those orbitals of the Mo_6X_8 cluster of this symmetry and which are outward pointing hybrids of the X_8 cube which will interact with the M atom orbitals. We have used[12] a similar illustrative technique to generate the orbitals of the CsCl and Cu_2O structures. With reference to **3**, the procedure we use to

(11) Stone, A. J. *Inorg. Chem.* **1981**, *20*, 563.

(12) Burdett, J. K.; Lin, J.-H. *Acta Crystallogr., Sect. B*, in press.

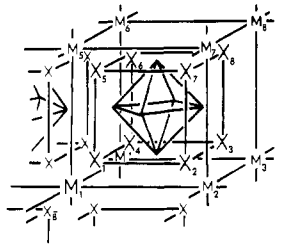

3

generate these orbitals is described as follows. M atoms 1–8 are translationally equivalent. The interaction between M(8) and X(8) is translationally equivalent to that between M(1) and X($\bar{8}$). However, only the boldly labeled atoms in **3** are included in our calculation. Thus we can simulate the sum of the M(1)–X($\bar{8}$) and M(8)–X(8) interactions by adding the corresponding off-diagonal element of the secular determinant for this interaction to that between the atoms M(1) and X(8) both of which do appear in the calculation on MMo_6X_8. This may be done for all M–X pairs, such that the metal (M) atoms orbitals have off-diagonal terms linking them with all eight X atoms of the cube. Thus the M atom *appears* to be cubally eight-coordinate, and each X atom *appears* to be four-coordinate (by three X and one M atom). Most easily appreciated from Figure 4 is the strong destabilization of M(ns,np) levels in forming MMo_6X_8. A somewhat smaller stabilization occurs for Mo_6X_8 orbitals of the same symmetry. The d-orbital region of the diagram remains virtually intact since direct Mo–M interaction is small due to their large mutual separation. The HOMO is the same e_g orbital as found in the $Mo_6X_8^{4-}$ molecular diagram and at this geometry contains no M atom character.

In the actual structure of MMo_6X_8 the inner cube and octahedron have been rotated within the outer cube of M atoms. Figure 5 shows the effect of such a distortion on the orbitals of the structure. The most dramatic change is associated with the largely M located empty a_{1g} and t_{1u} antibonding combinations between M and X_8. The t_{1u} level splits into orbitals of $a_1 + e$ symmetry as the rotation to the real structure proceeds. All four levels drop rapidly in energy. A similar effect associated with the filled bonding orbitals is less easy to see in Figure 5, but a corresponding destabilization of such occupied orbitals is associated with this motion. Energetically the d-orbital manifold remains virtually intact. The reasons for a loss of M–X bonding orbital stabilization and loss of M–X antibonding orbital destabilization on rotation are easy to see. In **4** and **5** we see the effect of rotation of the Mo_6X_8

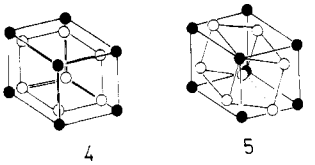

4 5

cube on the overlap of the frontier orbitals of this fragment with the cube of M orbitals. This loss of overlap between the orbitals on M and X atoms in general positions results in a calculated 2.6-eV destabilization of the structure on rotation by 20°. Our result, apparently not in agreement with experiment, is then that the observed, distorted structure is less stable than the ideal one. However, we have restricted ourselves to pseudomolecular calculations so far. How does the result change if we recognize that the species is really an infinite solid and we should include energetically interactions between the contents of one unit cell and the next?

Band Structure Calculations

Our fragment-within-the-solid orbitals descrie the level structure at the point Γ in the Brillouin zone. Their major

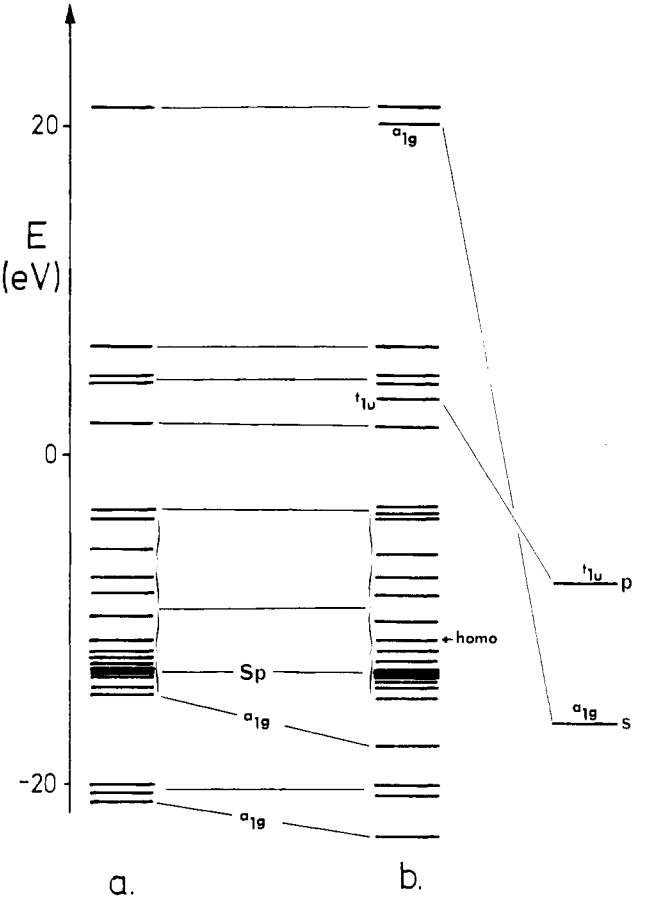

Figure 4. Generation of the fragment-within-the-solid orbitals for $PbMo_6S_8$ (b) from the molecular orbital diagram for Mo_6S_8 (a) by including translationally equivalent interactions between Pb and S atoms only. Only orbitals of a_{1g} or t_{1u} symmetry may shift as the interaction is switched on. The scale of the diagram is such that only the energy shifts of the bonding a_{1g} orbitals are clear to see. (The solid block of orbitals represent a collection of sulfur 3p orbitals. Since the energies of the levels are close together, a single line does not always represent a single orbital or degenerate set of orbitals.)

appeal is that, as in Figure 4, we are able to see quite clearly how the level structure of the pseudosolid is built up. This is difficult to do in other ways. However, even though these orbitals represent the orbital structure at this single, high-symmetry point in the zone, it is not to be assumed that the total energy of the solid or energy changes on distortion are accurately described by considering this point only. In principle we need to integrate the energy over the Brillouin zone in order to achieve this. In practice the "special points" method[13] of Baldareschi and of Chadi and Cohen is very useful. For the case of filled bands (i.e., nonmetals) then, the energy evaluated at a single **k** point, or small collection of **k** points is often a good approximation to the total energy. For the present primitive cubic case (the $\phi = 0°$ structure) evaluation at ($^1/_4$, $^1/_4$, $^1/_4$) will be sufficient. For the real, distorted, structure then the points ($^1/_4$, $^1/_4$, $^1/_4$) and ($^1/_4$, $^1/_4$, $-^1/_4$) weighted in the ratio 1:3 will analogously describe the energetics of the now rhombohedral structure.[14]

In our calculations all interactions between the atoms of one unit cell and those of neighboring ones are included. Some of these we shall find to be energetically quite important.

(13) (a) Baldareschi, A. *Phys. Rev. B* **1973**, *7*, 5212. (b) Chadi, D. J.; Cohen, M. L. *Phys. Rev. B* **1973**, *8*, 5744.

(14) In fact because our system is metallic with partially filled bands, the special points method is not strictly applicable. However, the large energy changes on distortion, as we shall see, are due to filled levels lying deeper than E_F, and so this approximation is not at all bad in this instance.

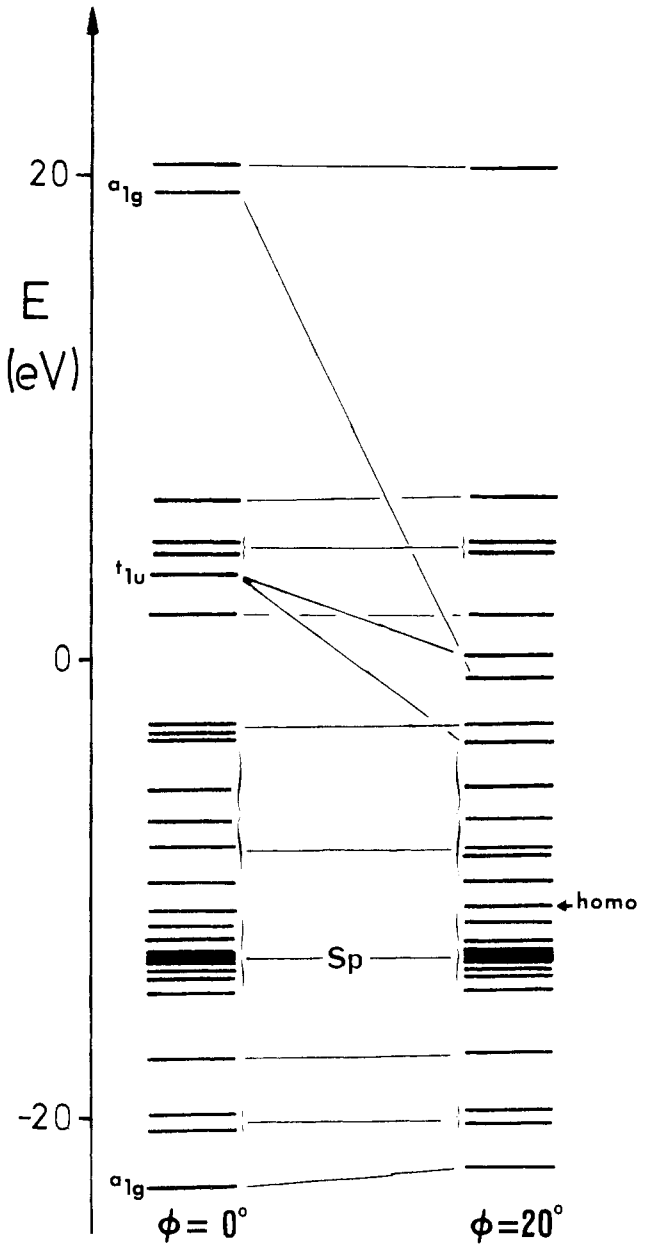

Figure 5. Fragment-within-the-solid orbitals (from Figure 4) showing the effect of rotation of the Mo_6S_8 unit around a threefold axis of the Pb_8 cube. Note that the major energy changes are associated with the orbitals which changed energy in Figure 4.

Mo_6 Cluster. The only really obvious difference between the molecular calculation and the band structure result is that the outward-pointing orbitals of the Mo_6 unit shift in energy as a result of interactions with neighboring octahedra (Figure 6). One of the t_{1u} orbitals is by symmetry antibonding at the point Γ and experiences a large destablization. Small stabilizations are found for the a_{1g} and e_g frontier orbitals. The predominantly d orbitals appear to be mainly nonbonding between adjacent octahedra and are little shifted in energy compared to the molecular calculation. It is then these higher energy, unoccupied, outward-pointing orbitals that experience the largest dispersion in **k** space (not shown) and also the largest energy changes on rotating the Mo_6 octahedron (Figure 6). There are however stabilizing interactions of a somewhat weaker sort between the occupied (largely d) orbitals of the octahedra, which are not as obvious as these from our diagram. Numerically we calculate a stabilization energy of 0.22 eV on going to the solid from the free unit for the idealized structure, a somewhat higher value for the real geometry. It is within these rather weak metal–metal interactions that the

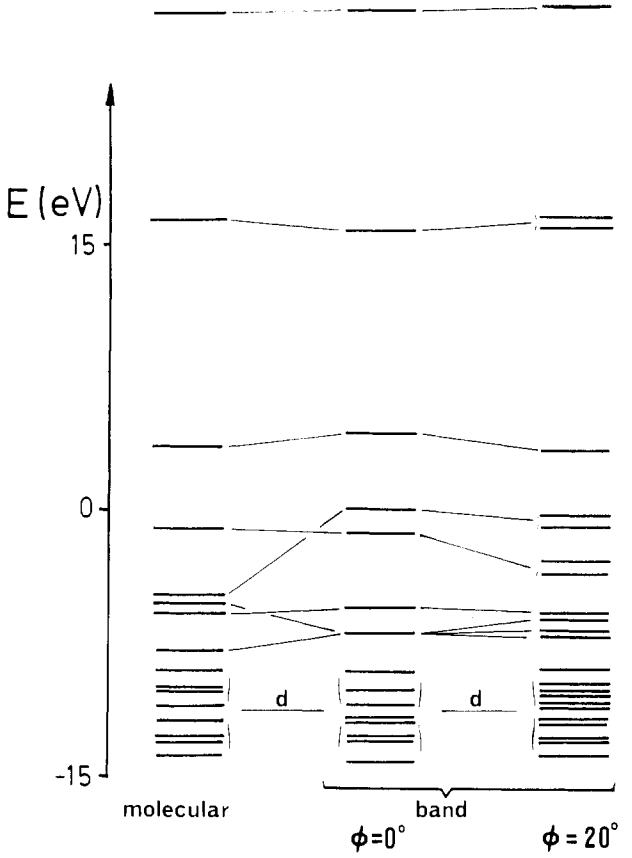

Figure 6. Band structure result at the point Γ in the Brillouin zone for the Mo_6 octahedron part of the Chevrel phase structure. Note the rather small energy changes involved on rotation compared to those of Figure 5.

explanation of the superconductivity properties probably lies. For an electronic configuration corresponding to Mo_6^{12+} this unit experiences a calculated destabilization on rotation by 20° of about 1 eV per unit cell for the idealized case of **1** where the Mo atoms lie in the facial planes of the cube. For the real structure, where the Mo atoms project out of the cube somewhat, the energy change is a little smaller (0.54 eV).

S_8 Cube. Because of the relatively large intracube S–S distance of 3.458 Å, the orbital diagram for molecular X_8 consists of a pair of groups of levels at the approximate energies of the S3s and S3p orbitals. The intercube S–S distance in the $\phi = 0°$ structure is significantly shorter and so this electronic state of affairs changes in the band structure with the effect of intercube interactions being larger than intracube ones (Figure 7a). All g orbitals of the X_8 cube are stabilized and all u orbitals destabilized at the point Γ in the Brillouin zone. Because of the interaction between one cube and another, these bands also experience high dispersion in **k** space. Figure 7b shows the levels along the symmetry line Λ linking Γ(0, 0, 0) and R($^1/_2$, $^1/_2$, $^1/_2$), which includes the special point ($^1/_4$, $^1/_4$, $^1/_4$). Both Γ and R possess the full holohedral symmetry; at points in between, the symmetry has been reduced and is not able to support a triply degenerate representation. The most interesting results concerning the orbital structure of this fragment are the energetic changes which occur on rotating the cube around one of its threefold axes. As Figure 7a shows, intercage interactions are relieved on rotation. The largest energy changes are, as expected, associated with the stabilization of the intercage antibonding orbitals (u symmetry in the isolated cube); somewhat smaller is the destabilization of their bonding counterparts. Smaller intercage interactions in the rotated geometry are also indicated by the somewhat smaller dispersion of these levels in **k** space. Overall for an

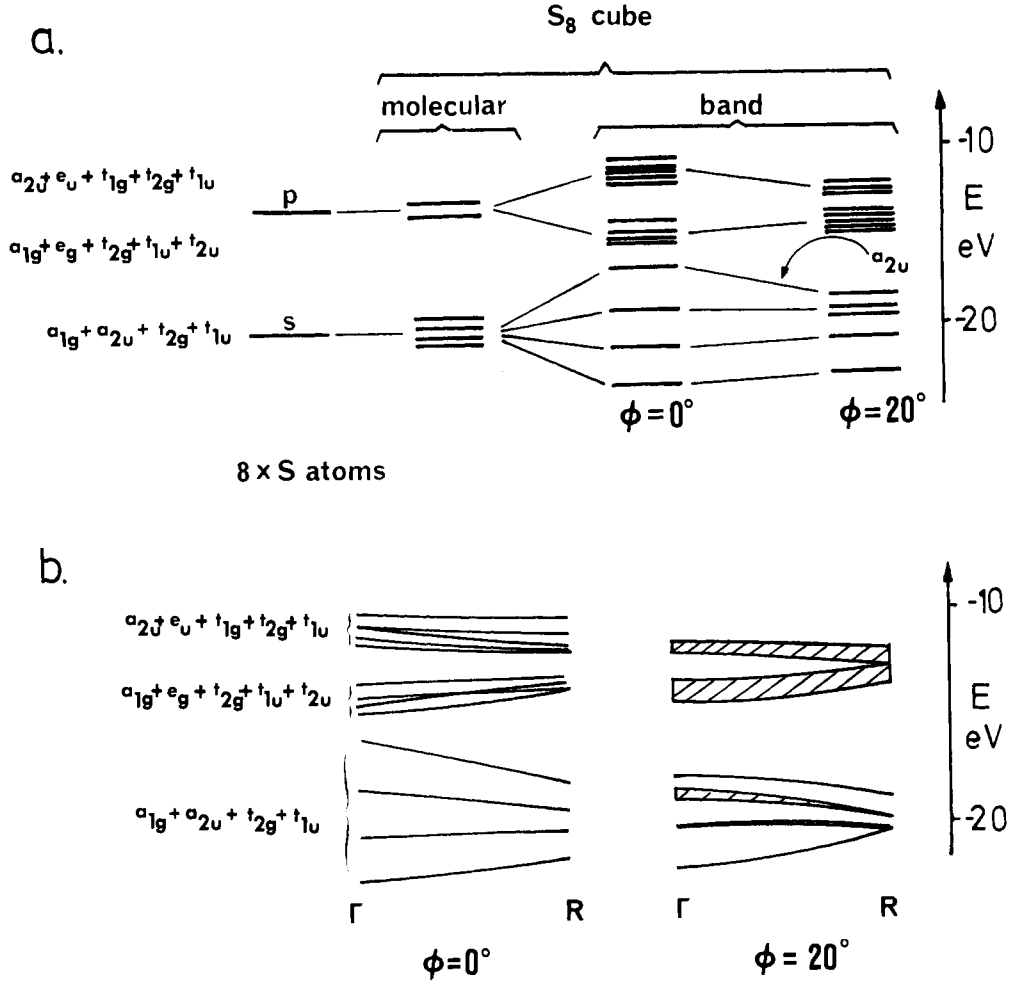

Figure 7. (a) Band structure results for an S_8 cube showing the level changes at Γ on rotation and (b) part of the band structure along the symmetry line Λ connecting Γ(0, 0, 0) and R($^1/_2$, $^1/_2$, $^1/_2$). The behavior on rotation for the orbitals of the MX_8 or MM'_6X_8 cluster on rotation are extremely similar. (The energies of the levels are often close together. A single line therefore does not always represent a single energy level on the diagram.)

S_8^{16-} cube the energy is dramatically lowered on rotation as this collection of closed shell units adjusts their mutual orientation so as to minimize the repulsions between them. In this way the geometrical change is strongly connected with our way of viewing the geometries of van der Waals molecules and solids.[15] Rather than assume that the relative orientation of two partners is set by the location of an energy minimum in the van der Waals attractive potential, we have pointed out that the geometry adopted is the one where the nonbonded repulsions of the system are minimized. At the special point ($^1/_4$, $^1/_4$, $^1/_4$), we find a dramatic 12 eV stabilization of S_8^{16-} on rotation for the idealized structure and 6 eV for the real structure. Half of this stabilization energy in each case arises from the orbitals of a_{2u} symmetry. One of these is shown in **6**. Interestingly, a rotated structure is found[5c] in Mo_6Se_8

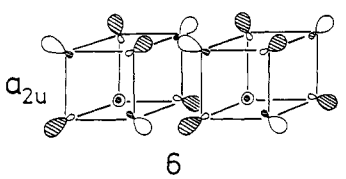

6

where the M atom is missing. In order to confirm our picture of dominant intercage interactions, we have repeated these band structure calculations as a function of intercage separation and find that indeed the effect decreases in importance as this structural parameter increases. Our model for the rotation therefore is different from the initial one of Anderson et al.,[16] which stressed intercluster Mo–Mo interactions and their later[3] conclusions, in accord with those Mattheis and Fong,[7] which stressed the maximization of intercluster Mo(d)–X(p) interactions. A piece of supporting evidence is presented below.

MX_8 and MMo_6X_8. Above we showed that pseudomolecular calculations on these Chevrel phases indicated that the nonrotated geometry was more stable than the observed, twisted one by about 2.6 eV. Band structure calculations on those systems, however, show a stabilization similar to that found for the S_8^{16-} unit itself and for exactly analogous reasons, namely, adjustment of the structure to relieve intercage X_8 repulsions. We calculate a minimum energy rotated structure for a turn angle of 25.0 ± 0.2°, which is very close to those observed (25.8° in $PbMo_6S_{7.5}$ and 25.6° in $PbMo_6Se_8$).

Effect of M on the Turn Angle. Our conclusion above was that the X_8 cubes rotated away from the ideal structure so as to avoid fierce mutual nonbonded repulsions between them. Clearly this repulsion will increase with increasing charge on the cubal unit. By replacing the M = Pb atom with a more electropositive pseudoatom (i.e., one with smaller H_{ii} values), we find that the X atom charge does indeed increase and that commensurately the calculated turn angle increases from 25.0 ± 0.2° to 27.5 ± 0.2°. This result may have an interesting application. As we mentioned above, these systems are often

(15) Burdett, J. K. *J. Chem. Phys.* **1980**, *73* 2825.

(16) See ref 6 in ref 7.

Table I. Atomic Parameters

	orbital exponents			H_{ii}, eV		
atom	s	p	d[a]	s	p	d
S	1.817	1.817		−20.0	−13.3	
Mo	1.7	1.7	4.95 (0.4876), 1.6 (0.7205)	−8.66	−5.24	−11.5
Pb	1.853	1.853		−16.5	−7.90	

[a] Double-ζ form, coefficients in parentheses.

high-temperature (up to 15 K) superconductors. However, if the lead atoms in $PbMo_6S_8$ are gradually replaced with the more electropositive europium, the superconductivity disappears.[17] $EuMo_6S_8$ itself becomes superconducting on the application of pressure.[18] Superconductivity in these systems is almost certainly associated with the overlap of d orbitals associated with adjacent pairs of molybdenum atom octahedra as suggested by Fischer.[4] On replacement of Pb by Eu, it is not too hard to envisage a larger turn angle of the Mo_6X_8 units with accompanying loss of Mo–Mo interunit interaction. This might be a very interesting example of structural control of such electrical properties.

Defect Structures. 7 shows the result of a population

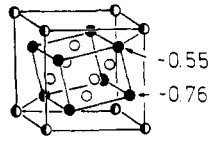

7

analysis of the molecular orbital calculation on the pseudomolecule MMo_6X_8 in the rotated geometry. The same trend is found for the charges from a band structure calculation averaged over the special points. Note that the atomic charges on the inequivalent X atoms are not equal. The two atoms in the special position have a smaller negative charge than those in the general position. In a defect structure in which one of the electronegative X atoms is missing, then by analogy with similar ways[19,20] of viewing site preferences in molecules, the lowest energy structure will result when the least negative site is vacated. This is actually what is observed experimentally; MMo_6X_7 and MMo_6X_6 structures are missing one or both "special position" X atoms. We calculate the energy of the MMo_6X_7 pseudomolecule to be 0.8 eV more stable with the vacancy in the special compared to general position. From the band structure calculations averaged over the special points, the corresponding figure is 1.87 eV.

This is a manifestation of a reasonably general molecular rule of thumb[19] that, given the choice, the more electronegative atoms in a structure will occupy the sites of lowest coordination number (e.g., $Cl(F)_3$ and not $F(Cl)(F)_2$). The X atoms in the special position have four "normal" linkages (three to Mo atoms, one to an M atom). The X atoms in the general position are "less coordinated" with, in addition to three "normal" MoX linkages, one longer M–X linkage. This conclusion however is not in accord with the suggestion by Delk and Sienko[4b] that in the mixed species $PbMo_6(S_{1-x}Se_x)_8$ the less electronegative selenium atoms preferentially occupy the general-position sites.

Acknowledgment. This research was supported by the National Science Foundation under Grant NSF DMR 8019741. We also thank the donors of the Petroleum Research Fund, administered by the American Chemical Society, for their partial support of this research, Dr. J. D. Thompson for useful conversations, and Professor R. Hoffmann for some valuable comments and criticisms.

Appendix

The distances used in the calculations on an idealized $PbMo_6S_8$ geometry where the Mo atoms lie in the facial planes of the cube were X–X = (S–S) = 3.67 Å, Mo–Mo = 2.60 Å, and M–M = (Pb–Pb) = 6.679 Å. For calculations on the "real" geometry, the distances were S–S = 3.458 Å, Mo–Mo = 2.717 Å, and Pb–Pb = 6.675 Å. The extended Hückel parameters are given in Table I. The band structure program was written by M.-H. Whangbo, to whom we are grateful for permission to use it.

Note Added in Proof. Our suggestion concerning the lack of superconductivity in $EuMo_6S_8$ may be only part of the story. A rhombohedral to triclinic phase transformation in this system at 110 K has been reported: Baillif, R.; Dunand, A.; Muller, J.; Yvon, K. *Phys. Rev. Lett.* **1981**, *47*, 672.

(17) Fischer, Ø.; Decraux, M.; Roth, S.; Chevrel, R.; Sergent, M. *J. Phys. C* **1975**, *8*, L474.
(18) Such an observation implies that the superconductivity is not spoiled by the proximity of the paramagnetic europium ion to the Mo_6 cluster but by some other effect.
(19) Burdett, J. K. "Molecular Shapes"; Wiley: New York, 1980.
(20) See, for example: Hoffmann, R.; Howell, J. M.; Rossi, A. *J. Am. Chem. Soc.* **1976**, *98*, 2484.